

Current statistics for transport through rectangular and circular billiards

Almas F. Sadreev

L.V. Kirensky Institute of Physics, Krasnoyarsk 660036, Russia

Department of Physics and Measurement Technology, Linköping University, S-581 83 Linköping, Sweden

Astaf'ev Krasnoyarsk Pedagogical University, Krasnoyarsk 660049, Russia

(Received 22 October 2003; revised manuscript received 27 February 2004; published 15 July 2004)

We consider the statistics of currents for electron (microwave) transmission through rectangular and circular billiards. For the resonant transmission the current distribution is describing by the universal distribution [A. I. Saichev *et al.*, *J. Phys. A* **35**, L87 (2002)]. For the more typical case of nonresonant transmission the current statistics reveals features of the current channeling (corridor effect) interior of the billiard. The numerical statistics is compared with analytical distributions.

DOI: 10.1103/PhysRevE.70.016208

PACS number(s): 05.45.Mt, 05.60.Gg, 73.23.Ad

I. INTRODUCTION

Recently the statistics of the scattering wave function and currents for electron (microwave) transmission through chaotic billiards was considered [1–3]. The statistics was based on the fact that the scattering function can be described a complex Gaussian random field $\psi = u + iv$ with the correlation $\langle uv \rangle$ dependent on the conductance and measure of the openness of the billiard. Such a scattering function can be given as a random superposition of the plane waves obeying the boundary conditions (the modified Berry function) [4–7].

The scattering function interior of the billiard can be superposed of the eigenfunctions of the billiard. Although the coefficients of superposition are not random, which is different from the Berry function [8], nonetheless superposition of the Gaussian random fields is also a complex Gaussian random field [9,10]. It allowed us to derive analytically the distribution functions for the scattering function [1], currents [2], and nodal points (vortices) [6,11,12]. These distributions were observed as numerically [4,5,11] as well as experimentally for the microwave transmission [13,14].

Surprisingly, the transmission through an integrable billiard is more complicated in comparison to the chaotic billiard. The reason is that the eigenfunctions of the integrable billiard do not obey the Gaussian distribution. The effect of channeling of transport currents (the current terminated leads attached to a billiard) is bright example of peculiar distributions for transmission through the rectangular billiard [4,15]. The channeling of currents is a consequence of the almost crystal order of nodal points [5,15]. Since the nodal points are centers of current vortices [5,16–18], the transport currents are to flow between rows of the vortices as in “corridors.” For a computation of current flows one can separate vortical bound currents and unbound currents which are terminated at the leads (transport currents) [19]. However, it is hardly possible to separate the transport and vortical currents in experiments. Therefore the statistics of the current density interior of the integrable billiard is a subject of consideration of present paper. The main result is that the current statistics shows the features related to the current channeling except for the case of resonant transmission.

The interplay between the symmetries of billiards and leads implies the selection rules for the coefficients of expansion

of the scattering function over the eigenstates of the billiard. The selection rules strongly reduce the number of eigenstates participating in transmission through the billiard. Effectively this number is about from 1 to a few as was shown numerically [4,5]. For transmission through chaotic billiards this number as a rule exceeds 10 which differs from transmission through integrable billiards.

II. TRANSMISSION THROUGH THE RECTANGULAR BILLIARD

A billiard can be opened by attaching leads to some exterior reservoirs and a stationary current through the billiard is induced by applying suitable voltages to the reservoirs. We consider leads as stripes attached normally to the billiard as shown in Fig. 1. The numerical procedure of the solution of the Helmgoltz equation

$$-\nabla^2 \psi = \epsilon \psi \quad (1)$$

describing transmission through a billiard is well known. Here we use dimensionless energy $\epsilon = E/E_0$, $E_0 = \hbar^2/2m^*d^2$

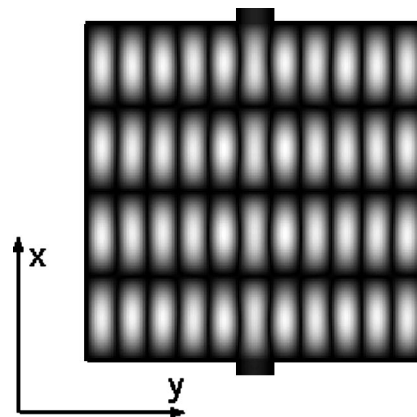


FIG. 1. The scattering function $|\psi(x,y)|$ for resonant transmission through a squared billiard with energy $\epsilon \approx \epsilon_{11,4} = 13.52$ and numerical lengths $N_x = N_y = 400$. The numerical width of the leads $d = 40$. The hopping matrix element between the leads and the billiard is chosen as 0.9.

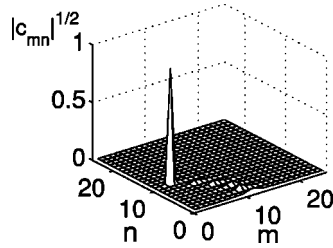


FIG. 2. The coefficients of expansion of the scattering function over the eigenstates (2).

where d is the width of the leads. In terms of E_0 we define also the eigenenergies of the billiard. In order to provide resonant transmission we imply hopping matrix elements $t < 1$ connecting the billiard and the leads [4,5,20].

Let us consider a rectangular billiard with lengths L_x, L_y and eigenfunctions obeying the Dirichlet boundary conditions as

$$\psi_{mn}(x, y) = \phi_m(x)\phi_n(y) = \frac{2}{A} \sin(m\pi x/L_x) \sin(n\pi y/L_y), \quad (2)$$

where $m=1, 2, 3, \dots, n=1, 2, 3, \dots, A=L_x L_y$, and the eigenenergies

$$\epsilon_{mn} = d^2 \pi^2 \left(\frac{m^2}{L_x^2} + \frac{n^2}{L_y^2} \right). \quad (3)$$

A. Resonant transmission

Tuning the incident energy to be resonant to the eigenenergy of the billiard $\epsilon \approx \epsilon_{mn}$ we can achieve a situation that the scattering function is to be very close to the corresponding eigenstate ψ_{mn} interior of the billiard. In Fig. 1 one can see that for $\epsilon \approx \epsilon_{11,4}$ the scattering function almost exactly follows the eigenfunction $\psi_{11,4}$. In the squared billiard there is the second degenerated eigenstate $\psi_{4,11}(x, y)$ which related to the first one by a rotation 90° . As seen from Fig. 1, a minimum of the second degenerated eigenstate is located near leads, which diminishes participation of this state in the transmission.

Quantitatively a measure of the resonant transmission can be given by the coefficients of expansion of the scattering function over the eigenstate (2) interior of the billiard:

$$\psi(x, y) = \sum_{m,n} c_{m,n} \phi_m(x) \phi_n(y). \quad (4)$$

Figure 2 shows that the contribution of the eigenstate $m=11, n=4$ is dominant in the scattering function. In order to resolve the contributions of different eigenstates to the scattering function in Fig. 2, we plotted the squared roots of the coefficients $|c_{mn}|^{1/2}$.

We consider the statistics of the local current density,

$$\mathbf{j}(\mathbf{x}, \mathbf{y}) = \text{Im}(\psi^* \nabla \psi), \quad (5)$$

interior of the billiard numerically computed as histograms. For microwave transmission this current is the Poynting vector [13]. A pattern of current flow for the resonant transmis-

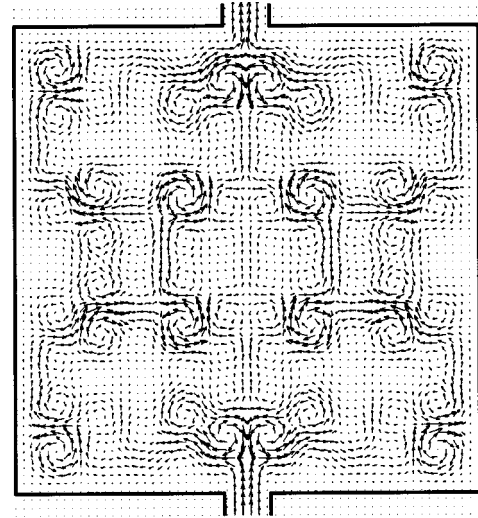


FIG. 3. The current density $\mathbf{j}(x, y)$ for resonant transmission through a squared billiard at the same parameters as given in Fig. 1.

sion is shown in Fig. 3. One can see that the pattern basically consists of vortical currents.

Figure 4 shows the numerical results for the statistics of the current density $P(j)$ and its components $P(j_x), P(j_y)$ for the resonant transmission.

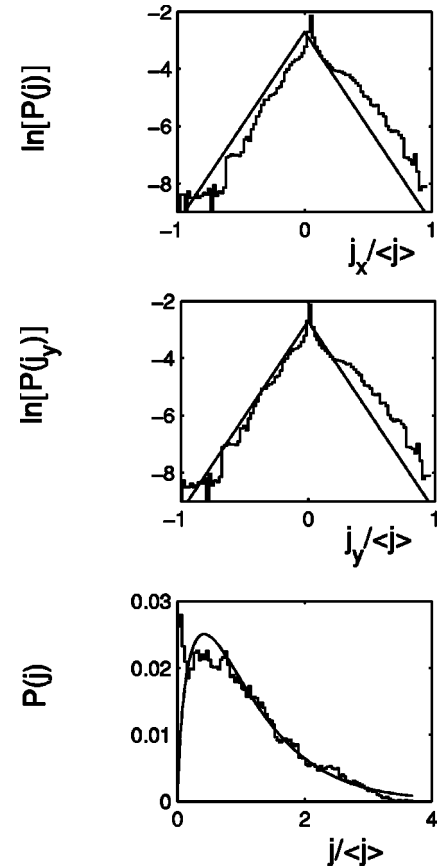


FIG. 4. Statistics of the current density $P(j)$ (bottom) and its components $P(j_x)$ and $P(j_y)$ for resonant transmission. The current distributions (6) and (7) are shown as solid lines.

These numerical results are compared with the current distributions derived in [2] for transport through chaotic billiards,

$$P(j_\alpha) = \frac{\pi}{4\langle j \rangle} \exp\left(-\frac{\pi|j_\alpha|}{2\langle j \rangle}\right), \quad (6)$$

$$P(j) = \frac{\pi^2 j}{4\langle j \rangle^2} K_0\left(\frac{\pi j}{2\langle j \rangle}\right), \quad (7)$$

where $\alpha=x,y$, $K_0(x)$ is the modified Bessel function of the second kind, and the average means

$$\langle \dots \rangle = \frac{1}{A} \int_A d^2\mathbf{r} \dots, \quad (8)$$

where A is the area to be sampled. In our case it will be area of the cavity, but in principle it could be any area that one may wish to diagnose. From Fig. 4 one can see qualitative agreement between the numerical results for the resonant transmission through the rectangular billiard and formulas (6) and (7) for the case of transmission through chaotic billiards.

In order to understand this agreement let us present the scattering function interior the billiard as

$$\psi = \psi_0 + \tilde{\psi}, \tilde{\psi} = \sum_{mn} c_{mn} \psi_{mn},$$

where ψ_0 is the resonant eigenfunction with $|c_0| \approx 1$ and ψ_{mn} are nonresonant eigenfunctions with the coefficients c_{mn} shown in Fig. 2 as weak background $|c_{mn}| \ll 1$. Then we can approximate the probability current as

$$\mathbf{j} \approx \text{Im}(c_0^* \psi_0 \nabla \tilde{\psi} + c_0 \tilde{\psi}^* \nabla \psi_0). \quad (9)$$

Therefore the probability current flows only because of the background $\tilde{\psi}$ which can be considered as random noise in accordance with Fig. 2.

B. Nonresonant transmission

Then it follows that, if effectively a very restricted number of eigenstates participates in transmission (say, 2 or 3), the current distribution can substantially differ from the results shown in Fig. 4. In order to achieve this case we can choose the incident energy between two resonant states as shown in Fig. 5(a) by a cross. Then, one can expect that mainly these resonant states will participate in transmission roughly equally while other eigenstates can be ignored. The coefficients of expansion (4) plotted in Fig. 5 for the nonresonant transmission confirm this assumption.

Figure 6 shows the current density for the nonresonant transmission shown in Fig. 5. One can see that the current flows into the interior of the rectangular billiard by the regular way in “corridors” parallel to the transport axis x , which is different from Fig. 3. The corridors are related by the symmetry $y \rightarrow -y$. There are three main different corridors. Moreover, there are regions of depleted currents between the corridors. In other words, we can say that the density currents are channeling the interior of the billiard. The channel-

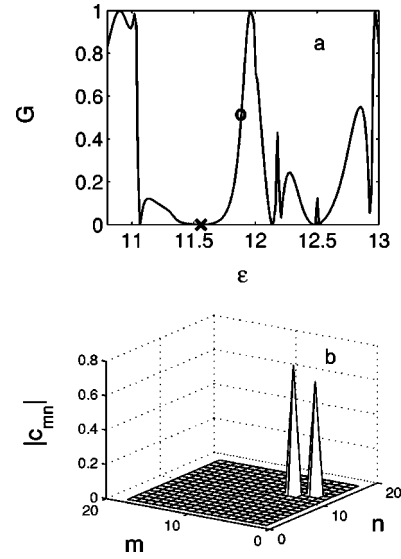


FIG. 5. (a) Transmission through the rectangular billiard with numerical sizes $N_x=500$, $N_y=400$, $d=40$. The hopping matrix element between leads and billiards is equal to 1. (b) The coefficients of the expansion (4) for the nonresonant transmission shown in (a) by a cross at $\epsilon=11.56$. Two coefficients $c(5,13)=0.592-0.412i$ and $c(3,14)=0.315-0.607i$ are dominated in the transmission.

ing effect is a purely geometrical one because of the regular arrangement of the vortices. As shown in Fig. 7 the current statistics $P(j_x)$ correlates with these observations where the x axis is directed along the transport. One can see three distinctive plateaus: one for positive j_x and two for negative j_x responsible for the corridors. Moreover, the distribution $P(j_x)$ shows multiple additional plateaus which are responsible for the current corridors which are not resolved in Fig. 6. As seen from Fig. 7 the distribution $P(j_y)$ is substantially different from $P(j_x)$.

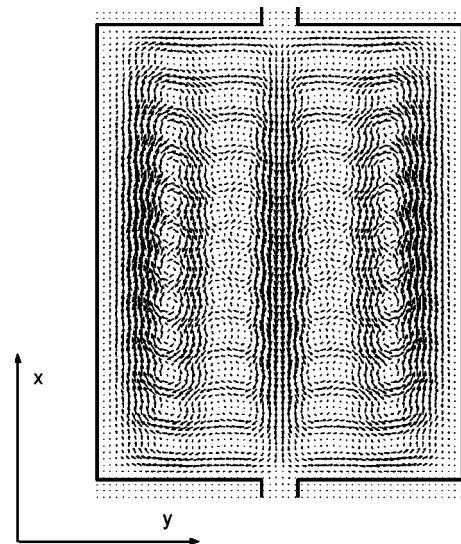


FIG. 6. The density current $\mathbf{j}(x,y)$ for the nonresonant transmission through a rectangular billiard with parameters given in Fig. 5(a).

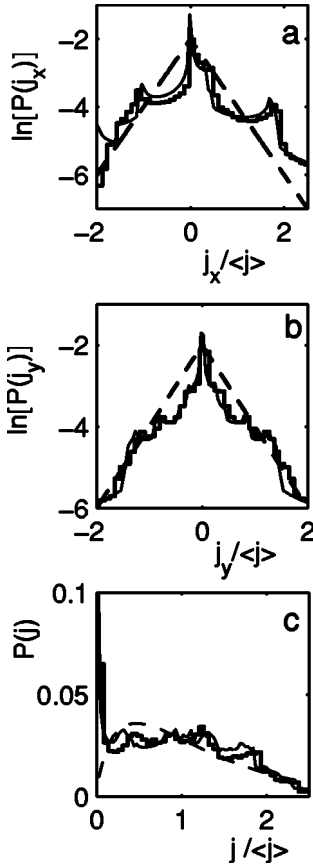


FIG. 7. Statistics of the probability current density $P(j)$ (c) and its components $P(j_x)$ and $P(j_y)$ (a), (b) for nonresonant transmission for the energy shown in Fig. 5(a) by a cross. The current distribution (12) is shown by a thin solid curve. The current distributions for chaotic billiards (6) and (7) are shown by the dashed curves.

For a description of numerical current statistics for nonresonant transmission we keep in the expansion (4) only two contributions in correspondence to Fig. 5(b):

$$\psi(x, y) = C_1 \psi_{mn}(x, y) + C_2 \psi_{m'n'}(x, y), \quad (10)$$

where the coefficients C_1, C_2 are complex. Specific values of the coefficients are given in Fig. 5. Then it follows from Eq. (2) that the x th component of the probability density current takes the form

$$j_x(x, y) = j_0 u(x) v(y),$$

$$u(x) = \phi_m(x) \phi_{m'}'(x) - \phi_m'(x) \phi_{m'}(x),$$

$$v(y) = \phi_n(y) \phi_{n'}(y), \quad (11)$$

where the constant j_0 is related to the normalization coefficients of the scattering function and the prime is the derivative. Using the properties of the δ function we can write the distribution function for j_x :

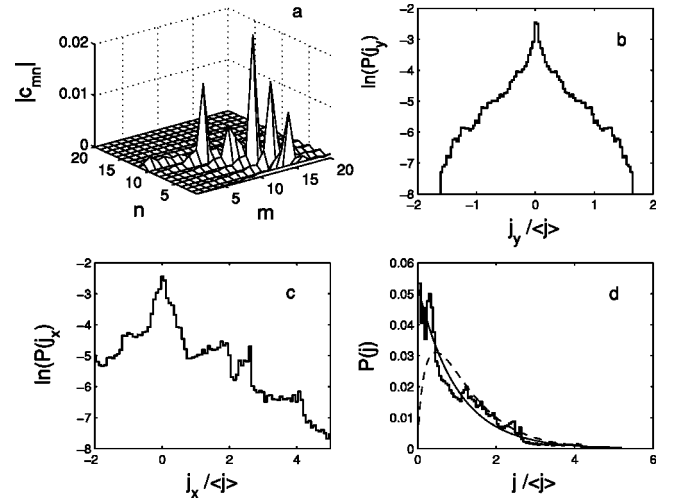


FIG. 8. (a) The coefficients of expansion (4) for nontransmission through a rectangular billiard with numerical sizes given in Fig. 5 for $\epsilon=11.8$ shown in Fig. 6 by a circle. Distributions of probability current density $P(j)$ (d) and its components $P(j_x)$ and $P(j_y)$ (b), (c). For comparison the current distribution (7) is shown by the dashed line and the Poisson distribution $P(j)=(1/\langle j \rangle)\exp(-j/\langle j \rangle)$ is shown by the solid line.

$$P(j_x) = \int_A dx dy \delta(\gamma - u(x)v(y)) = \int_0^{L_x} dx \frac{1}{u(x) v'|_{v=\gamma/u(x)}}, \quad (12)$$

$\gamma = j_x/j_0$. The same expression can be derived for $P(j_y)$ where

$$j_y(x, y) = j_0 u(x) v(y),$$

$$u(x) = \phi_m(x) \phi_{m'}(x),$$

$$v(y) = \phi_n(y) \phi_{n'}'(y) - \phi_n'(y) \phi_{n'}(y). \quad (13)$$

Integration over x in Eq. (12) can be performed numerically.

In the above-considered numerical case the eigenmodes with quantum numbers $m=5, n=3$ and $m=3, n=4$ mainly participate in the quantum transmission. Substituting these numbers into Eq. (11) and consequently performing numerical integration in Eq. (12) we obtain the distribution $P(j_\alpha), \alpha=x, y$, which is shown in Fig. 7(a) by the thin solid lines. One can see good agreement with numerical statistics.

Finally, we present the current statistics for transmission in which more than two eigenstates of the rectangular billiard participate in the transmission shown in Fig. 8. The corresponding incident energy is shown in Fig. 4(a) by a circle.

III. TRANSMISSION THROUGH A CIRCULAR BILLIARD

A. Resonant transmission

In a similar way we consider transmission through a circular billiard. The transmission probability is shown in Fig. 9 with numerical sizes given in the figure caption.

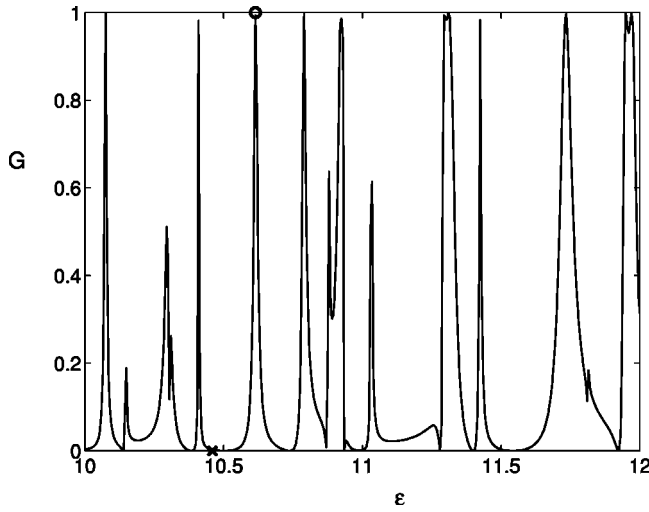


FIG. 9. The transmission probability vs the energy (a) for transmission through a circular billiard with numerical radius $R=250$ and lead width $d=30$. The hopping matrix elements between the leads and billiard is equal to 0.95.

As for resonant transmission through the rectangular billiard [Eq. (4)] the scattering function interior of the billiard can be expanded over the eigenfunctions of the closed circular billiard,

$$\psi(x,y) = \sum_{m,n} c_{m,n} J_m(k_{mn}r) \exp(im\phi), \quad (14)$$

where k_{mn} are zeros of the Bessel functions. As is seen from Fig. 10 for the energy shown by a circle in Fig. 9 the eigenfunction $J_4(k_{47}r)\cos(4\phi)$ dominates in the expansion (14).

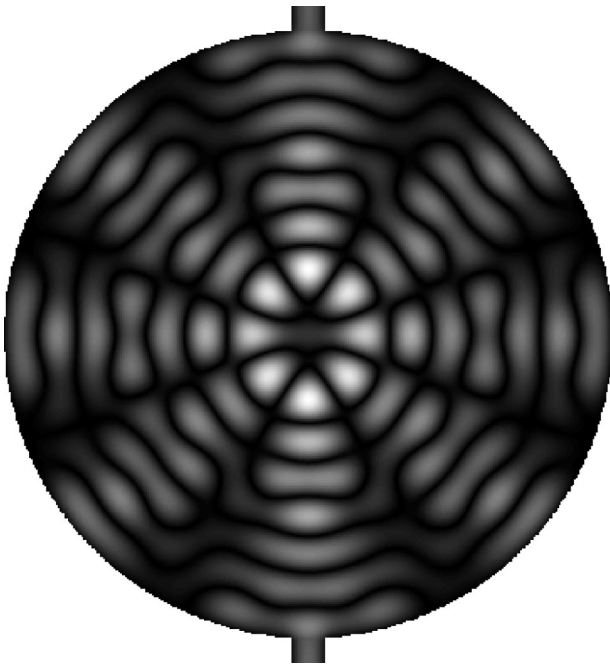


FIG. 10. The scattering function $|\psi(x,y)|$ for the resonant transmission through a circular billiard with energy $\epsilon=10.615 \approx \epsilon_{4,7} = (d/R)^2 k_{4,7}^2$ and numerical sizes given in Fig. 9.

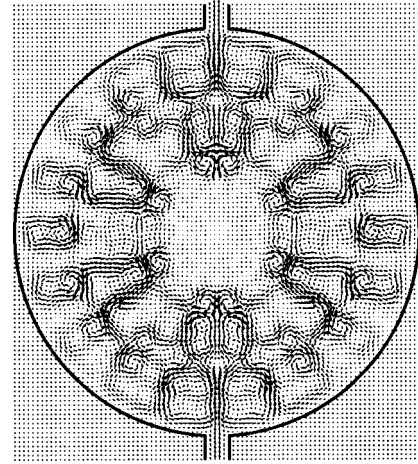


FIG. 11. The current density $\mathbf{j}(x,y)$ for resonant transmission through a circular billiard at the same parameters as given in Fig. 9 and $\epsilon=10.615$.

The current flow for the resonant transmission is shown in Fig. 11. One can see from Fig. 11 that the probability current flow behaves as shown in Fig. 3. Therefore we can expect that current distributions can be described by formulas (6) and (7). In fact, Fig. 12 confirms that.

B. Nonresonant transmission

Let us consider nonresonant transmission, for example, taking the incident energy $\epsilon=10.45$ between two resonant peaks as shown in Fig. 9 by a cross. The corresponding pattern of current flow shown in Fig. 13 demonstrates the tangential “corridor” effect. The numerically calculated current

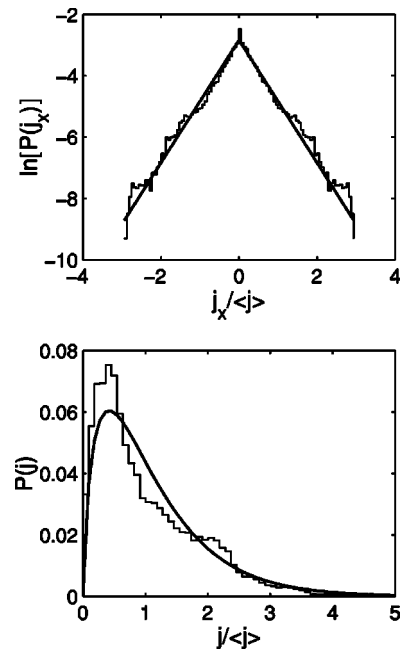


FIG. 12. The current statistics for resonant transmission through a circular billiard with parameters given in Figs. 9 and 10 compared with the current distributions (6) and (7) shown as solid lines.

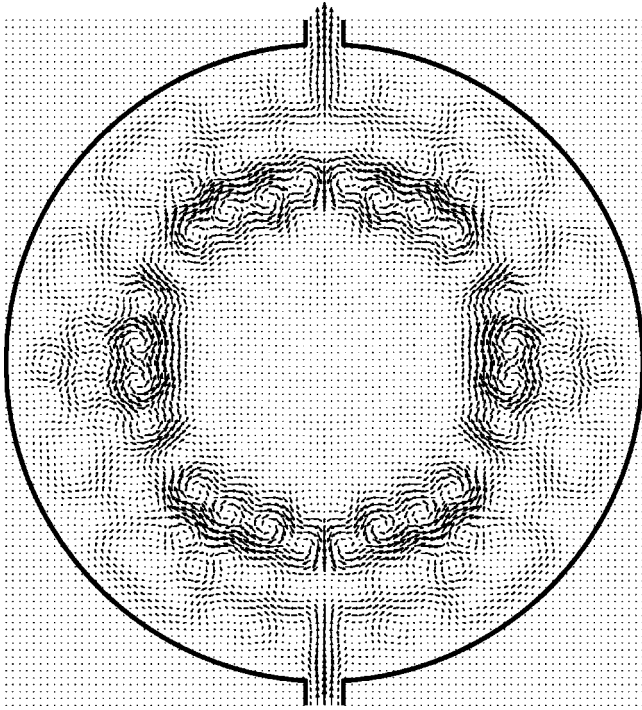


FIG. 13. The probability current density for the nonresonant transmission through a circular billiard with numerical radius $R = 250$ and lead width $d = 30$ for $\epsilon = 10.45$. The hopping matrix elements between the leads and billiard is equal to 0.95.

statistics $P(j)$ is shown in Fig. 14. One can see a sharp peak in the distribution related to this “corridor” effect.

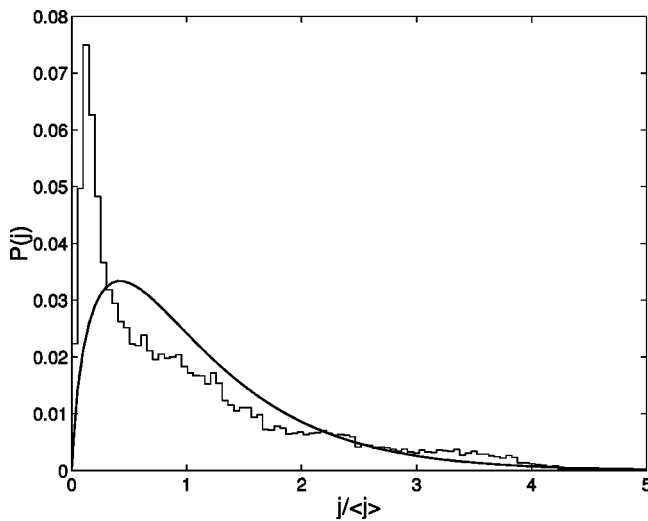


FIG. 14. The current distribution $P(j)$ of the flow pattern shown in Fig. 13 compared with formula (7).

IV. SUMMARY AND DISCUSSION

We have considered numerically and analytically the probability current distributions for quantum transmission through the two typically integrable billiards: rectangular and circular ones. This consideration is also related to the microwave transmission for which the current distributions can be measured directly [13]. For resonant transmission with the transmission probability near unity the scattering function is close to those eigenfunction of the billiard the eigenenergy of which is resonant to the energy of the incident electron (Figs. 1 and 10). Obviously, in the expansion of the scattering function over the eigenfunction interior of the billiard the resonant eigenfunction dominates. Contributions of different eigenfunctions form small but wide random noise as shown in Fig. 2. Since these nonresonant functions are responsible for the probability current in accordance with Eq. (9), it is not surprising that the current distributions can be described by the distributions derived for current interior of the chaotic billiards [2].

For the case of nonresonant transmission a few (as a rule two or more) of the eigenfunctions of the billiard dominate in the scattering function interior of the billiard. The probability current density (11) is defined mainly by these eigenfunctions. As a result, the current distributions are deeply nonuniversal. However, the most interesting result is that the probability density current interior of the billiard demonstrate the effect of corridor flowing as shown in Figs. 6 and 13. For the rectangular billiard the “corridors” are directed along the transmission axis (the x axis) and the distribution $\ln[P(j_x)]$ displays a few plateaus responsible for these corridors as seen from Fig. 7. The numerical current distributions agree with formulas derived for the case of two eigenfunctions contributed to the scattering function. For transmission through the circular billiards the corridors are tangential as shown in Fig. 13.

Moreover, we note the remarkable similarity between the current distributions and the level statistics of the nearest level separations. For the chaotic billiards the level statistics follows the Wigner-Dyson distribution which is quite similar to the current distribution (7). The last is shown by the thin solid line in Fig. 8 for the typical nonresonant transmission. One can see that the distribution (7) is far from the numeric. For the integrable billiards the level statistics of the nearest level separations follows the Poisson formula $P(x) = \exp(-x)$. We see from Fig. 8 that the current distribution for nonresonant transmission through the integrable billiard is well described by the Poisson distribution [21].

ACKNOWLEDGMENTS

I am grateful to K.-F. Berggren, U. Kuhl, and H.-J. Stöckmann for discussions and Anton Starikov for assistance in computer simulations of the transmission through billiards. This work was supported by RFBR Grant No. 04-02-16408.

- [1] H. Ishio, A. I. Saichev, A. F. Sadreev, and K.-F. Berggren, Phys. Rev. E **64**, 056208 (2001).
- [2] A. I. Saichev, H. Ishio, A. F. Sadreev, and K.-F. Berggren, J. Phys. A **35**, L87 (2002).
- [3] P. W. Brouwer, Phys. Rev. E **68**, 046205 (2003).
- [4] K.-F. Berggren, A. F. Sadreev, and A. Starikov, Nanotechnology **12**, 562 (2001).
- [5] K.-F. Berggren, A. F. Sadreev, and A. A. Starikov, Phys. Rev. E **66**, 016218 (2002).
- [6] M. V. Berry, J. Phys. A **35**, 3025 (2002).
- [7] M. V. Berry and H. Ishio, J. Phys. A **35**, 5961 (2002).
- [8] M. V. Berry, Philos. Trans. R. Soc. London, Ser. A **287**, 237 (1977).
- [9] W. Feller, *An Introduction to Probability Theory and its Applications* (Wiley, New York, 1971).
- [10] M. I. Tribelsky, Phys. Rev. Lett. **89**, 070201 (2002).
- [11] M. V. Berry and M. R. Dennis, Proc. R. Soc. London, Ser. A **456**, 2059 (2000).
- [12] A. I. Saichev, K.-F. Berggren, and A. F. Sadreev, Phys. Rev. E **64**, 036222 (2001).
- [13] M. Barth and H.-J. Stöckmann, Phys. Rev. E **65**, 066208 (2002).
- [14] Y.-H. Kim, M. Barth, and H.-J. Stöckmann, Phys. Rev. B **65**, 165317 (2002).
- [15] K.-F. Berggren, K. N. Pichugin, A. F. Sadreev, and A. Starikov, JETP Lett. **70**, 403 (1999).
- [16] J. O. Hirschfelder, J. Chem. Phys. **67**, 5477 (1977).
- [17] M. V. Berry, in *Physics of Defects*, edited by R. Balian *et al.* (North-Holland, Amsterdam, 1981).
- [18] P. Exner, P. Šeba, A. F. Sadreev, P. Streda, and P. Feher, Phys. Rev. Lett. **80**, 1710 (1998).
- [19] A. F. Sadreev and K.-F. Berggren, Phys. Rev. E (to be published).
- [20] A. F. Sadreev and I. Rotter, J. Phys. A **36**, 11413 (2003).
- [21] K. J. Ebeling, *Statistical Properties of Random Wave Fields in Physical Acoustics: Principles and Methods* (Academic, New York, 1984).